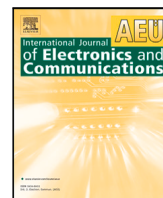




Contents lists available at ScienceDirect

Int. J. Electron. Commun. (AEÜ)

journal homepage: [www.elsevier.com/locate/aeue](http://www.elsevier.com/locate/aeue)

Short communication

## Cavity-stacked filter in CLAF-SIW technology for millimeter waves

Cleofás Segura-Gómez<sup>a</sup>,\*, Andrés Biedma-Pérez<sup>a</sup>, David Santiago<sup>b</sup>,  
Ángel Palomares-Caballero<sup>c</sup>, Iván Arregui<sup>b</sup>, Miguel A. Gómez Laso<sup>b</sup>, Pablo Padilla<sup>a</sup><sup>a</sup> Department of Signal Theory, Telematics and Communications, Research Centre for Information and Communication Technologies (CITIC-UGR), University of Granada, Calle Periodista Rafael Gómez Montero, 2, Granada, 18071, Spain<sup>b</sup> Smart Cities Institute (ISC), Department of Electrical, Electronic and Communication Engineering, Public University of Navarra (UPNA), Arrosadia, s/n, Pamplona, 31006, Spain<sup>c</sup> Institut d'Electronique et des Technologies du numérique (IETR), UMR CNRS 6164, INSA Rennes, Rennes, 35700, France

## ARTICLE INFO

## Keywords:

Cavity-stacked filters  
Chebyshev filter  
CLAF-SIW technology  
Electromagnetic bandgap  
Millimeter waves  
Planar technologies

## ABSTRACT

This work presents the design of a cavity-stacked bandpass filter (BPF) using contactless air-filled substrate integrated waveguide (CLAF-SIW) technology for millimeter-wave frequencies. This technology is a variant of air-filled SIW technology, incorporating contactless techniques. It enables the reduction of dielectric losses in SIW filters while supporting multilayer structures with robust assembly. The cavity-stacked filter topology allows for very good frequency responses with a reduced footprint and no transitions needed. As an example, a 4th-order Chebyshev bandpass filter composed of four stacked cavities, coupled through irises, is shown. The iris layers are fabricated by metallizing the slot edges of a PCB, while the cavity layers are implemented using CLAF-SIW. The filter has been designed and manufactured to provide a passband response from 36 GHz to 37.5 GHz. A good agreement between measurement and simulation has been achieved. The losses in the proposed CLAF-SIW filter are primarily due to the metal roughness of the low-cost commercial laminates used.

## 1. Introduction

The increase in operating frequencies for communication systems in recent years has introduced new challenges in device design. While millimeter-wave frequencies enable higher capacity and data rates in communications, they also make the manufacturing process more complex. In particular, this paper focuses on the design of bandpass filters (BPFs), which are essential for discriminating frequency channels and preventing external noise or interference [1].

Some of the main desired features for BPFs at millimeter-wave frequencies are a reduced footprint, low losses, and cost-effectiveness. This allows for more streamlined integration into a complete system. One of the technologies that can meet these requirements is substrate integrated waveguide (SIW) [2]. Several SIW BPF designs have been proposed for millimeter-wave frequencies [3–10]. However, various drawbacks have been identified in previous works such as substrate losses [6] or the use of costly manufacturing processes, such as LTCC [4, 5] to ensure loss-free assembly of layers. The issue of increasing dielectric losses at higher frequencies has been addressed through SIW variants such as the empty-SIW (E-SIW) [11] and the air-filled SIW (AF-SIW) [12]. Both technologies eliminate the dielectric region where

propagation occurs within the waveguide, thereby minimizing this source of losses. Several BPF designs in E-SIW [11] and AF-SIW [13,14] have been proposed for operation in the millimeter-wave frequency band. However, since these technologies are multilayer, good electrical contact between layers must be ensured, for example by using glue or soldering [11,15]. Otherwise, at these frequencies, any assembly tolerance can lead to leakage losses between layers. Additionally, another inherent complexity of previous BPF designs is the need to implement transitions to the host technology of the BPFs due to their in-line configuration.

In order to mitigate the aforementioned issues, an effective method for creating waveguides on printed circuit boards (PCBs) using electromagnetic band-gap (EBG) structures was presented in [16]. This technology, called contactless air-filled SIW (CLAF-SIW), incorporates substrate removal like E-SIW and AF-SIW, while also providing enhanced assembly robustness due to the use of EBG. Several devices have been implemented in CLAF-SIW, such as a temperature sensor based on a resonator at 2.57 GHz [17] and phase shifters based on periodic structures [18]. However, its application in filters for millimeter-wave

\* Corresponding author.

E-mail addresses: [cleofas@ugr.es](mailto:cleofas@ugr.es) (C. Segura-Gómez), [abieper@ugr.es](mailto:abieper@ugr.es) (A. Biedma-Pérez), [david.santiago@unavarra.es](mailto:david.santiago@unavarra.es) (D. Santiago), [Angel.Palomares-Caballero@insa-rennes.fr](mailto:Angel.Palomares-Caballero@insa-rennes.fr) (Á. Palomares-Caballero), [ivan.arregui@unavarra.es](mailto:ivan.arregui@unavarra.es) (I. Arregui), [mangel.gomez@unavarra.es](mailto:mangel.gomez@unavarra.es) (M.A.G. Laso), [pablopadilla@ugr.es](mailto:pablopadilla@ugr.es) (P. Padilla).<https://doi.org/10.1016/j.aeue.2025.155725>

Received 11 November 2024; Accepted 13 February 2025

Available online 22 February 2025

1434-8411/© 2025 Elsevier GmbH. All rights are reserved, including those for text and data mining, AI training, and similar technologies.

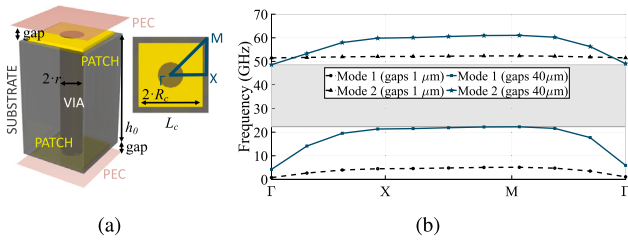


Fig. 1. Design of an EBG structure. (a) Unit cell layout, and (b) dispersion diagram. Dimensions (in mm):  $R_c = 0.37$ ,  $L_c = 0.90$ ,  $r = 0.15$ ,  $h_0 = 1.524$ .

frequencies has not yet been exploited.

This paper presents the potential of CLAF-SIW technology for achieving a low-cost, low-loss, and transition-free filter using a stacked-cavity configuration. The work details the design and characterization of a CLAF-SIW BPF from 36.0 GHz to 37.5 GHz with a 4 percent fractional bandwidth. The document is organized as follows. Section 2 explains the constraints of CLAF-SIW, the components used to build the filter, and its design method. Section 3 describes the experimental characterization of the filter, along with a discussion of the results and comparisons with other reported filters. Finally, Section 4 presents the conclusions.

## 2. CLAF-SIW bandpass filter design

In the design of BPFs in SIW, E-SIW, and AF-SIW technologies, in-line topologies are typically considered for feeding the filter structure [6,11,13]. Therefore, transitions from standard technologies, such as coaxial or rectangular waveguides, are required for system integration or frequency characterization. These transitions can be implemented in various ways, such as using a stepped rectangular waveguide [19] or a tapered microstrip [20]. However, using in-line topologies with ad-hoc transitions for BPFs introduces some disadvantages, such as an increase in footprint size, a reduction in component performance due to the required transitions, and the need for a calibration kit to achieve accurate device characterization. The BPF design proposed in this work leverages a stacked topology to mitigate all the issues associated with filters using in-line topology. CLAF-SIW technology is the most suitable technology for this type of filter with a stacked cavity topology, as it involves the use of a multilayer structure. Given the operating frequency range, inter-layer assembly tolerances become critical [21], but CLAF-SIW effectively mitigates potential leakage losses.

This section is divided into several subsections that describe the unit cell required for the CLAF-SIW structure [see Fig. 1], the filter design method, a filter design example, and a discussion on various effects that need to be considered in the CLAF-SIW cavities. An example of a stacked-laminate filter is shown in Fig. 2(a). The figure has a transparency to look through the filter structure and observe the different components that compose it. This type of filter consists of resonant cavities separated by coupling irises. Depending on the number of cavities, the order of the filter can be adjusted. In the case of the CLAF-SIW technology design, each element is designed on a laminate, so a new laminate is introduced for each cavity and for each iris. The design is based on commercial RO4003C laminates, meaning it is constrained by the available thicknesses of these laminates, with the height of each layer being fixed. For the cavity laminates, the thickness is 1.524 mm with a 35  $\mu\text{m}$  double-sided metallization, while for the iris laminates, the thickness is 0.813 mm with an 18  $\mu\text{m}$  double-sided metallization. Regarding the design process, it can be summarized in the following steps:

*Step 1.* Select the design laminates. This aspect determines the height of the cavities and the irises.

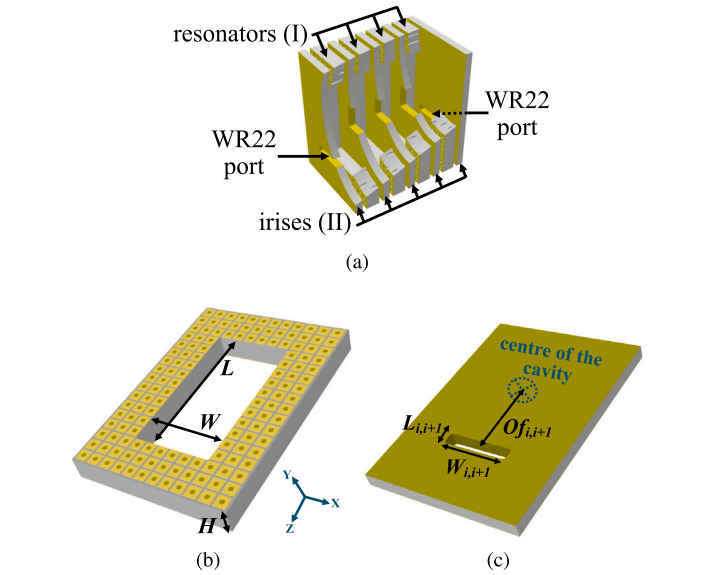
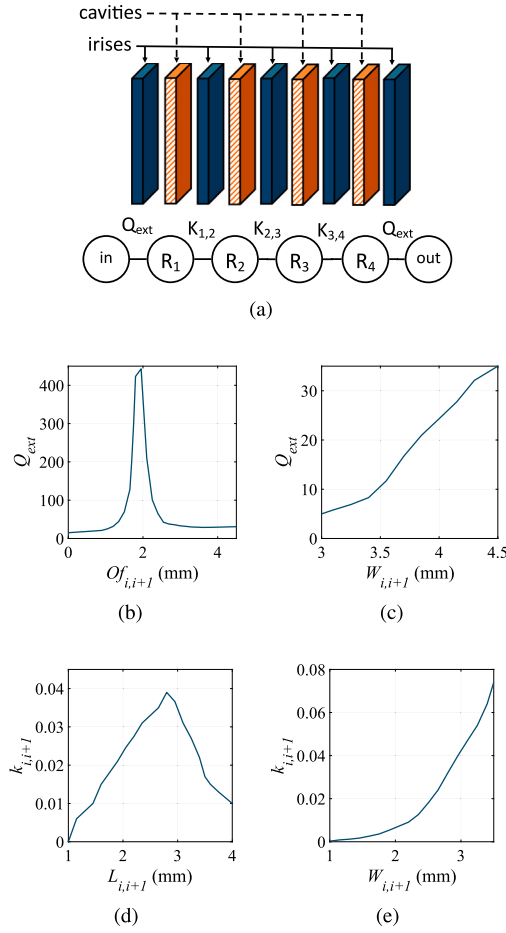


Fig. 2. Cavity-stacked filter in CLAF-SIW: (a) complete view, (b) resonant cavity layer (I), and (c) iris aperture layer (II).

- Step 2.* Establish an EBG unit cell for a stopband that includes the range of frequencies for the BPF.
- Step 3.* Select the order of the Chebyshev bandpass filter to calculate the required design parameters.
- Step 4.* Determine the dimensions of the CLAF-SIW cavity.
- Step 5.* Determine the dimensions of the irises to obtain the previously calculated design parameters.

### 2.1. EBG unit cell

As mentioned above, CLAF-SIW technology eliminates the leakage losses that can occur when assembling AF-SIW layers. These losses are due to gaps caused by mechanical tolerances between the layers, which may result in separations of up to 20  $\mu\text{m}$  [16]. To minimize these undesired effects, the metallized vias of the side walls are replaced by an EBG structure [16]. Leveraging the fact that the main structure is printed on a PCB, a double mushroom-like EBG structure is necessary to mitigate the leakage losses caused by the two possible gaps (upper and lower) created between the laminates employed to define the cavities and those used to implement the irises. This is illustrated in Fig. 1(a), where the double mushroom-like EBG is shown. This unit cell is formed by a metallized via inside the dielectric that joins a metal patch on the top face and a metal patch on the bottom face of the PCB. Its design is performed by adjusting the periodicity between unit cells (unit cell size), the ratio between unit cell and metal patch, and the ratio between unit cell and via. Additionally, the height and electrical permittivity properties of the laminate play a fundamental role in the propagation of modes within the unit cell, as detailed in [16]. The dispersion diagram produced by this EBG unit cell was obtained using the eigensolver of the CST Studio Suite and is shown in Fig. 1(b). The dispersion diagram allows us to identify the frequencies at which the electromagnetic field does not propagate inside the structure. The first mode that appears at low frequencies is the mode that propagates through the gap (if any) and is therefore controlled by the height of the gaps. The higher frequency mode, which is the one that propagates inside the dielectric, is controlled mostly by the laminate height, the ratio of via to unit cell, and the dielectric constant. More information about this unit cell type and its modes is provided by [16]. In this case, the designed EBG unit cell prevents electromagnetic field leakage between 22 GHz and 49 GHz for gaps up to 40  $\mu\text{m}$ , which are actually larger than the expected gaps in fabrication [16]. For smaller gaps, the stopband is even wider.



**Fig. 3.** Filter design: (a) Topology. Analysis of the external quality factor,  $Q_{ext}$ , and coupling coefficient between two stacked cavities,  $k_{i,i+1}$ , using CLAF-SIW  $TE_{102}$  resonators: (b)  $Q_{ext}$  varying  $O_{f,i+1}$  with  $W_{i,i+1} = 4.2$  mm and  $L_{i,i+1} = 0.80$  mm, (c)  $Q_{ext}$  varying  $W_{i,i+1}$  with  $L_{i,i+1} = 0.80$  mm and  $O_{f,i+1} = 3.24$  mm, (d)  $k_{i,i+1}$  varying  $L_{i,i+1}$  with  $W_{i,i+1} = 2.90$  mm and  $O_{f,i+1} = 0$  mm, and (e)  $k_{i,i+1}$  varying  $W_{i,i+1}$  with  $L_{i,i+1} = 2.70$  mm and  $O_{f,i+1} = 0$  mm.

## 2.2. Filter design method

The filter design method provides the dimensions of the filter layers. First, the operating  $TE_{pqn}$  mode must be selected, considering the trade-off between design robustness against manufacturing errors and the filter size [22]. To estimate the dimensions of the resonator, the following expression for rectangular waveguide technology is used [22]:

$$f_{0,pqn} = \frac{c}{2\pi} \sqrt{\left(\frac{p\pi}{W}\right)^2 + \left(\frac{q\pi}{H}\right)^2 + \left(\frac{n\pi}{L}\right)^2} \quad (1)$$

where  $c$  is the speed of light in free-space and  $W$ ,  $H$ , and  $L$  are the width, height, and length, respectively, of the effective CLAF-SIW resonator [see Fig. 2(b)]. These dimensions can be adjusted using a full-wave electromagnetic simulator taking into account the dimensions of the EBG unit cell described in Section 2.1. Furthermore, for the resonant cavity, it must be considered that its height is influenced by the double gap (upper and lower), which may occur due to assembly tolerances. Finally, it is necessary to determine the coupling coefficients between the resonators,  $k_{i,i+1}$ , and the external quality factor,  $Q_{ext}$ , as detailed in [23]:

$$k_{i,i+1} = \frac{BW}{\sqrt{g_i \cdot g_{i+1}}}, \quad i = 1, \dots, N-1 \quad (2)$$

$$Q_{ext} = Q_{1,N} = \frac{g_0 \cdot g_1}{BW} \quad (3)$$

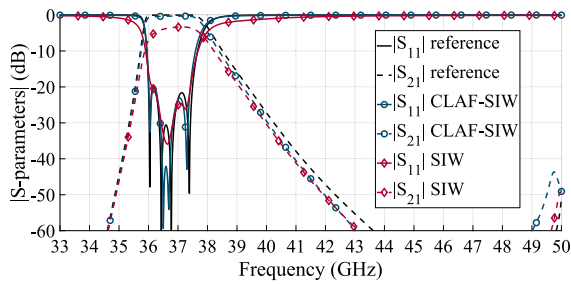
**Table 1**  
Dimensions (in mm) of the filter implemented in CLAF-SIW technology.

Element	Length (L)	Width (W)	Height (H)	Offset (Of)
Air cavity	9.700	5.100	1.624	–
Input/output irises ( $Q_{ext}$ )	0.809	4.221	0.849	3.242
Intermediate irises ( $k_{12}=k_{34}$ )	2.737	2.861	0.849	0
Central irises ( $k_{23}$ )	2.275	2.906	0.849	0

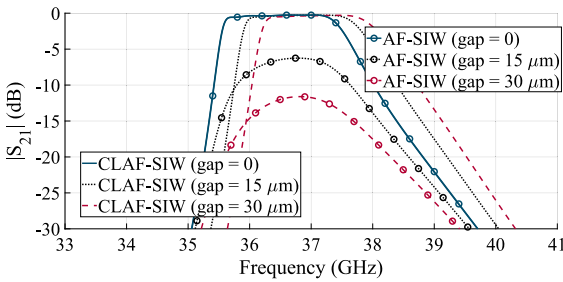
where  $BW$  is the fractional bandwidth,  $N$  is the order, and  $g_i$  are the normalized coefficients of the corresponding low-pass prototype. To implement the required values of  $k_{i,i+1}$  and  $Q_{ext}$ , iris apertures are used in the top and bottom walls of the resonators, allowing for the stacked configuration [see Fig. 2(c), which shows one of the iris apertures]. Fig. 3(a) schematically displays the stacked topology of the proposed filter. As an example for the  $TE_{102}$  mode (which will later be the selected one for the design example), Fig. 3(b) illustrates the large range of values that can be obtained for the  $Q_{ext}$  parameter as a function of the offset  $O_{f,i+1}$ , used to excite a cavity resonating mode. In Fig. 3(c), the variation of this parameter concerning the aperture width  $W_{i,i+1}$  is also shown. Additionally, Figs. 3(d) and 3(e) demonstrate how different values of  $k_{i,i+1}$  can be achieved by varying the aperture length  $L_{i,i+1}$  and its width  $W_{i,i+1}$ , respectively. It is important to note that, due to the field distribution of the  $TE_{102}$  resonant mode and the stacked configuration, the position of the iris or the aperture in the  $z$ -direction influences these parameters, thus determining the type of variations observed in the previous figures.

## 2.3. Performance of the cavity-stacked CLAF-SIW filter

To validate the proposed method for designing stacked filters in CLAF-SIW technology, a 4th order Chebyshev filter with a passband between 36 GHz and 37.5 GHz and in-band return loss better than 20 dB has been selected. Using (1)–(3), the values of  $k_{i,i+1}$  and  $Q_{ext}$  required to achieve the target response are calculated:  $Q_{ext} = 29.55$ ,  $k_{12} = k_{34} = 0.037$ , and  $k_{23} = 0.029$ . Additionally, to obtain a design robust against manufacturing errors without significantly increasing the cavity size, the  $TE_{102}$  mode has been used as the resonant mode, with  $W = 5.1$  mm and  $L = 9.7$  mm in the air cavity. As explained in [22], the use of a higher-order mode allows for an increase in the cavity size, which reduces the sensitivity to manufacturing errors. However, since the operating frequency of this device is maintained in the low range of the millimeter-waves, only a higher-order mode beyond the fundamental one is used to avoid enlarging the cavity unnecessarily and to maintain a low footprint. Therefore, using Fig. 3 and slight electromagnetic optimization, the dimensions of the filter detailed in Table 1 can be obtained. In order to compare the behavior of this device with its counterparts in other technologies, the filter has been also implemented in a stacked configuration of rectangular waveguide (referred to as the reference), CLAF-SIW, and SIW. It should be noted that the reference filter has slightly different dimensions (5.69 mm for the cavity width and 10.44 mm for the cavity length) to resonate at the same frequency. The height of all cavities remains unchanged, following the value  $H$  of Table 1. Comparing the main dimensions ( $L$ ,  $W$ ) of the reference filter with the ones of the CLAF-SIW cavity, we note that the latter is smaller, but the complete CLAF-SIW cavity requires three EBG unit cells on each side. The magnitude of the scattering (reflection and transmission) parameters of the reference filter and its implementations in CLAF-SIW and SIW are presented in Fig. 4(a). For a fair comparison, tolerance gaps have not been considered in the simulated results displayed in Fig. 4(a). It can be observed that the reflection and transmission parameters of the CLAF-SIW filter are practically identical to those of the ideal reference BPF. This indicates that the dielectric losses in the CLAF-SIW filter are virtually negligible. In contrast, the stacked SIW filter, where the air in the resonant cavities



(a)



(b)

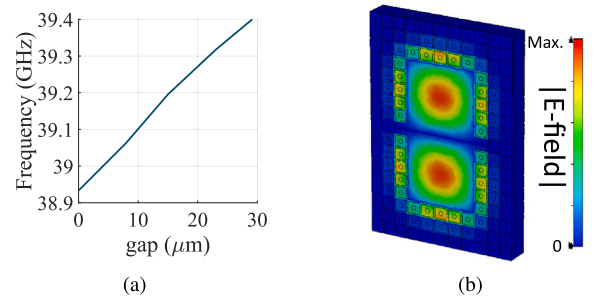
Fig. 4. S-parameters of the cavity-stacked filter: (a) Comparison of the ideal design with the CLAF-SIW filter and the equivalent SIW filter, and (b) comparison in transmission of the CLAF-SIW filter with the AF-SIW filter when the size of the tolerance gap varies.

has been replaced with dielectric, would exhibit higher losses, approximately 3 dB more. It is important to emphasize that the proposed filter design is free from spurious modes in the frequency band supported by the standard WR-22 waveguide ports, which ranges from 33 GHz to 50 GHz.

To complete the performance benchmark, Fig. 4(b) presents a comparison between the proposed CLAF-SIW filter and the corresponding AF-SIW filter (the same filter but without the EBG structure) as the size of the tolerance gaps increases. In the case of a zero gap, both filters exhibit the same transmission response over frequency. However, as the gap increases, the absence of EBG unit cells in the AF-SIW filter causes field leakage, resulting in non-negligible losses (around 6 dB) with just 15  $\mu\text{m}$  of gap size. In contrast, for the CLAF-SIW filter, an increase in the gap size up to 30  $\mu\text{m}$  leads to a slight shift in the operating band without causing noticeable transmission losses, as shown in Fig. 4(b). This demonstrates the low-loss performance and robustness of the proposed filter design during assembly at millimeter-wave frequencies. Moreover, a cavity-stacked filter design using CLAF-SIW technology becomes cost-effective since it eliminates the need of adhesive layers or soldering to mitigate tolerance gaps between layers.

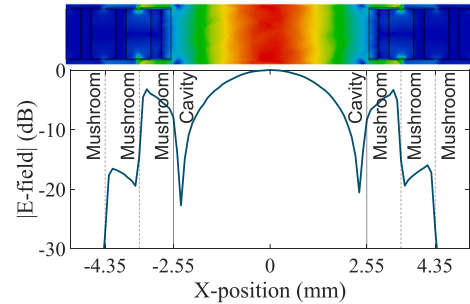
#### 2.4. Considerations on the CLAF-SIW cavity

As mentioned above, the presence of tolerance gaps in the CLAF-SIW filter causes a slight shift in the operating band. This is primarily due to the modification of the effective dimensions of the resonant cavity. Accurately determining the theoretical resonant mode frequency in a CLAF-SIW cavity using Eq. (1) is complex due to several factors. First, the resonant frequency differs from that in a perfect air-cavity because the effective dimensions in SIW are influenced by the spacing between the vias [24]. Additionally, the effective dimensions in AF-SIW are a combination of the remaining dielectric in the lateral zone and the central air zone [12]. Moreover, another factor affecting the resonant frequency of the CLAF-SIW arises when tolerance gaps are taken into account. Fig. 5(a) shows how, over a small range of tolerance gaps, the resonant frequency of a CLAF-SIW cavity shifts by about 0.5 GHz.

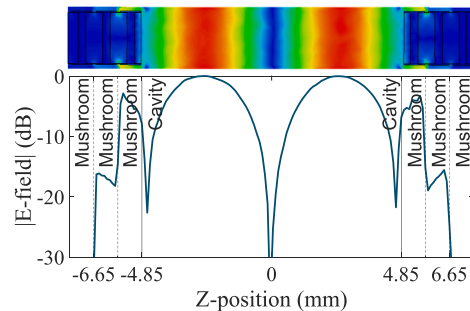


(a)

(b)



(c)



(d)

Fig. 5. Performance of the CLAF-SIW cavity: (a) Resonant frequency varying with gap size, and (b) E-field distribution. E-field distribution along the main dimensions of the cavity: (c) X-axis (or width), and (d) Z-axis (or length). Dimension:  $gap = 15 \mu\text{m}$ .

Fig. 5(b) illustrates how, for this tolerance gap, the electric field (E-field) can penetrate the first row of EBG unit cells, slightly perturbing the cavity mode. This occurs because the effective width and length of the CLAF-SIW cavity are modified. This can be most clearly seen in Figs. 5(c) and 5(d), which display the E-field distribution along the width and the length of the CLAF-SIW cavity, respectively. The size of the gap influences the E-field distribution at the first row of the EBG unit cell in the CLAF-SIW cavity. This effect determines the position of the null at the mushroom-cavity interface which is visible in the labeled vertical lines in Figs. 5(c) and 5(d). As the gap size increases, the position of these nulls shifts toward the center of the cavity, increasing the resonant frequency, as shown in Fig. 5(a). A similar effect can be observed for the cutoff frequency in waveguides implemented in CLAF-SIW [18].

### 3. Measured results and discussion

The different layers of the filter were fabricated and are shown in Fig. 6(a). Various views of the CLAF-SIW cavity-stacked filter are presented in Fig. 6(b). For the measurements taken using a vector network analyzer (VNA) R&S-ZVA67, two standard coaxial-to-WR-22 waveguide adapters were required, as displayed in the lower part of Fig. 6(b). The

**Table 2**  
Comparison with other filter designs in SIW and related technologies for Millimeter-wave frequencies.

Ref.	Freq. (GHz)/ BW <sup>a</sup>	Insertion losses (dB)	Configuration/ technology	Order	Size <sup>c</sup> / laminates	Design complexity
[6]	30/4%	2.74	in-line/SIW	4	$3.06 \times 1.78 \times 0.04/1$	High
[9]	42.2/4.6%	4.2	in-line/SIW	4	$2.44 \times 1.58 \times 0.08/1$	Medium
[10]	30.5/4.9%	1.3 <sup>b</sup>	in-line/SIW	N/A	$0.59 \times 0.39 \times 0.05/1$	Low
[13]	33/10%	1	in-line/AF-SIW	4	$1.87 \times 0.77 \times 0.28/5$	Medium
[14]	30/6%	1 <sup>b</sup>	in-line/AF-SIW	3	$2.46 \times 0.50 \times 0.15/3$	Low
This Work	36.75/4%	1.5	cavity-stacked/CLAF-SIW	4	$1.31 \times 1.29 \times 1.85/9$	Low

<sup>a</sup> Central frequency and fractional bandwidth.

<sup>b</sup> Minimum insertion losses.

<sup>c</sup> Size in terms of guided wavelength. Following axis of Fig. 2(b): “Y”(transmission direction) x “X” x “Z”.

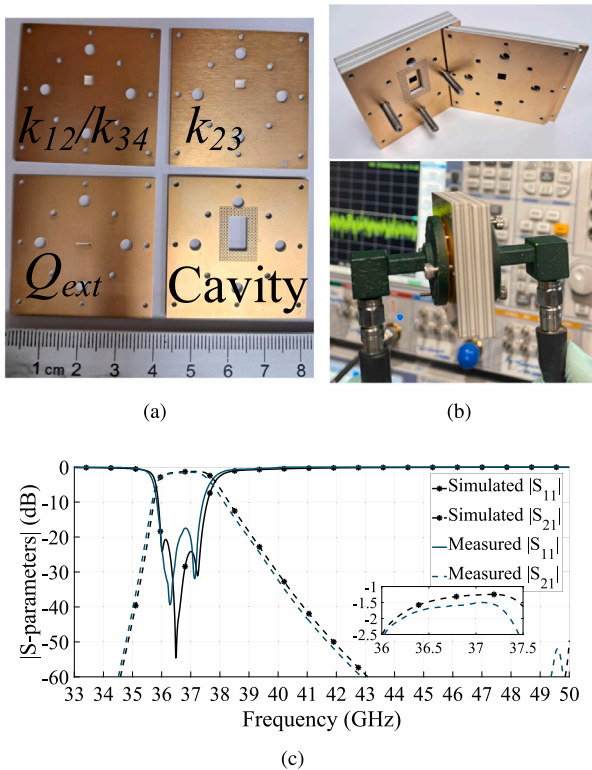


**Fig. 6.** CLAF-SIW cavity-stacked filter: (a) Forming layers, (b) assembly of the filter and setup, (c) simulated and measured S-parameters. Inset: detail of the insertion loss.

measured and simulated results are shown in Fig. 6(c). The simulations account for all sources of losses associated with the commercial RO4003C laminate, including dielectric losses from the substrate, metal losses due to copper conductivity, and losses due to a metal roughness (for the typical values of RO4003C laminate after processing). It is observed that the measured passband matches the one selected in the design method. Specifically, the reflection level in the measured results is slightly poorer than in the simulations, making some reflection zeros not easily recognizable. The differences between the simulated and measured results are mainly attributed to manufacturing tolerances, such as the actual gap size. As said above, the gap size slightly shifts the resonant frequency [see Fig. 5(a)] and, consequently the passband. However, the major problem is in the manufacturing tolerances of the smallest dimensions such as the separation between patches of the EBG unit cells or the input/output irises. They are minimized thanks to the use of the higher modes and the benefits provided by the CLAF-SIW technology. Therefore, there is good agreement between the simulation and measurement results across the frequency range, particularly in the slopes that define the transmission response of the filter. The measured passband shows a  $|S_{11}|$  below  $-15$  dB, where the reflection zeros

approximately align with the simulated results. The measured insertion losses are around 1.5 dB, dominated by metal roughness, as dielectric and metal conductivity losses (excluding roughness) are estimated to be around 0.4 dB in the passband according to the simulations. Roughness losses are expected in this frequency range as the skin depth decreases and approaches the surface roughness value, leading to a higher loss contribution. One way to reduce roughness losses is through polishing techniques [25].

In Table 2, the proposed CLAF-SIW filter is compared with other SIW-based filters from the literature that operate in the millimeter-wave frequency range, although with different BW (and it is well known that responses with narrower BW will inherently have higher insertion loss (IL)). The filter design presented in this work is the first to utilize CLAF-SIW technology, leveraging the advantages of this technology to implement a cavity-stacked configuration. This configuration has not yet been applied to SIW or AF-SIW filters in the millimeter-wave range, likely due to the lack of robustness provided by these technologies in multilayer assembly. Additionally, the proposed CLAF-SIW filter operates at a higher frequency while achieving a narrow-band response (4% BW) compared to the other filters in Table 2. When increasing the operating frequency, as in [9], the IL parameter increases significantly. In terms of IL, the filter in CLAF-SIW offers lower losses than the SIW filter based on conventional fabrication [6,9] and with the same BW, while avoiding the expensive LTCC fabrication. Moreover, it achieves similar IL to AF-SIW filters, without requiring transitions or the calibration kit needed in [13,14] and with a narrower BW. Despite the higher number of laminates used in this work, the cost is reduced as well as in the rest of the filters in Table 2 thanks to simple PCB manufacturing. Another advantage is the compactness by laminate stacking. In this aspect, this implies that increasing the filter order will only increase by multiples of the substrate thickness in the Y direction [see axis in Fig. 2(b)]. The other compared filters would need more space in the transmission direction as the width and length of the added resonators are greater than their height, which is marked by the substrate thickness. Another advantage concerning the proposed contactless filter is the re-usability of the cavities if a filter of another order is desired. Only the change of coupling iris laminates would be necessary, being beneficial for a mass production of the filter. In the case of the filters compared in Table 2, a change in their filter order would entail a redesign and fabrication of the complete filter without reusing any of its parts.

#### 4. Conclusion

In this work, a cavity-stacked filter using CLAF-SIW technology is proposed for millimeter-wave frequencies. By leveraging the advantages of CLAF-SIW in terms of tolerance handling in multilayer assembly, the proposed filter consists of nine layers combining cavities and aperture irises. A performance comparison of the CLAF-SIW filter with its implementation in SIW and AF-SIW has been conducted. It has been found that the cavity-stacked filter design in CLAF-SIW technology is superior to the other implementations, as it effectively

mitigates dielectric losses and leakage through the tolerance gaps. The proposed filter design was prototyped using commercial laminates and a cost-effective assembly process, which avoids the use of soldering or adhesive layers to ensure contact between the filter layers. The measured results are in good agreement with the simulations, providing a passband response centered at 36.75 GHz with a 4% BW. The proposed filter in CLAF-SIW provides the following main benefits: (i) robustness in the fabrication and assembly, (ii) low cost thanks to the PCB manufacturing process, (iii) directly compatible with standard waveguide technology without the need of ad-hoc transitions, (iv) relatively low insertion losses in the millimeter-wave frequencies and (v) compactness and straightforward redesign due to the cavity-stacked configuration and contactless feature. This work also shows that this filter and its design methodology are promising due to its cost-effective implementation and performance for filtering applications at millimeter-wave frequencies, where different frequency bands for wireless communications will be allocated.

### CRedit authorship contribution statement

**Cleofás Segura-Gómez:** Writing – review & editing, Writing – original draft, Visualization, Validation, Software, Resources, Methodology, Investigation, Formal analysis, Data curation, Conceptualization. **Andrés Biedma-Pérez:** Writing – review & editing, Writing – original draft, Visualization, Validation, Software, Resources, Methodology, Investigation, Formal analysis, Data curation, Conceptualization. **David Santiago:** Writing – review & editing, Writing – original draft, Visualization, Validation, Software, Resources, Methodology, Investigation, Formal analysis, Data curation, Conceptualization. **Ángel Palomares-Caballero:** Writing – review & editing, Writing – original draft, Visualization, Validation, Supervision, Software, Resources, Methodology, Investigation, Formal analysis, Conceptualization. **Iván Arregui:** Writing – review & editing, Writing – original draft, Visualization, Validation, Supervision, Software, Project administration, Methodology, Investigation, Funding acquisition, Formal analysis, Conceptualization. **Miguel A. Gómez Laso:** Writing – review & editing, Writing – original draft, Visualization, Validation, Supervision, Software, Project administration, Methodology, Investigation, Funding acquisition, Formal analysis, Conceptualization. **Pablo Padilla:** Writing – review & editing, Writing – original draft, Visualization, Validation, Supervision, Resources, Project administration, Methodology, Investigation, Funding acquisition, Formal analysis, Conceptualization.

### Declaration of competing interest

The authors declare the following financial interests/personal relationships which may be considered as potential competing interests: Cleofás Segura Gomez reports financial support was provided by Spain Ministry of Science and Innovation. Pablo Padilla de la Torre reports financial support, article publishing charges, equipment, drugs, or supplies, and travel were provided by Spain Ministry of Science and Innovation. Iván Arregui reports financial support, article publishing charges, equipment, drugs, or supplies, and travel were provided by Spain Ministry of Science and Innovation. Miguel A. Gomez Laso reports financial support, article publishing charges, equipment, drugs, or supplies, and travel were provided by Spain Ministry of Science and Innovation. Andrés Biedma Perez reports financial support was provided by Spain Ministry of Science and Innovation. If there are other authors, they declare that they have no known competing financial interests or personal relationships that could have appeared to influence the work reported in this paper.

### Acknowledgments

This work has been supported by grant TED2021-129938B-I00 funded by MCIN/AEI/10.13039/501100011033 and by the European Union NextGenerationEU/PRTR. It has also been supported by Grants PID2020-112545RB-C53, PID2020-112545RB-C54, PDC2022-133900-I00, and PDC2023-145862-I00, funded by MCIN/AEI/10.13039/501100011033 and by the European Union NextGenerationEU/PRTR. It has also been supported by Grant FPU20/00256 funded by MCIN/AEI/10.13039/501100011033 and by ESF Investing in your future.

### Data availability

No data was used for the research described in the article.

### References

- [1] Watanabe AO, Ali M, Sayeed SYB, Tummala RR, Pulgurtha MR. A review of 5G front-end systems package integration. *IEEE Trans Compon Pack Manuf Technol* 2021;11(1):118–33.
- [2] Wu K, Bozzi M, Fonseca NJ. Substrate integrated transmission lines: Review and applications. *IEEE J Microw* 2021;1(1):345–63.
- [3] Chen X-P, Wu K. Self-packaged millimeter-wave substrate integrated waveguide filter with asymmetric frequency response. *IEEE Trans Compon Pack Manuf Technol* 2012;2(5):775–82.
- [4] Shen T-M, Chen C-F, Huang T-Y, Wu R-B. Design of vertically stacked waveguide filters in LTCC. *IEEE Trans Microw Theory Tech* 2007;55(8):1771–9.
- [5] Huang X, Zhang X, Zhou L, Xu J-X, Mao J-F. Low-loss self-packaged Ka-band LTCC filter using artificial multimode SIW resonator. *IEEE Trans Circuits Syst II-Express Briefs* 2023;70(2):451–5.
- [6] Liu Q, Zhou D-F, Gong K, Wang J-H, Zhang D-W, Ma B-H. Dual- and triple-mode single-layer substrate-integrated waveguide filters based on higher-order modes for millimeter-wave applications. *IEEE Trans Circuits Syst II-Express Briefs* 2024;71(4):1994–8.
- [7] Wang L, Chen H, Li W, Gao L, Cai X, Fang Z, et al. A low-loss slow wave SIW bandpass filter with blind via-holes using TGV technology. *IEEE Microw Wirel Techn Lett* 2024;34(3):271–4.
- [8] Liu H, Chen L, Wu S, Mao M, Baxter H, Yang B, et al. A new electric coupling and its applications on millimeter-wave SIW filter with high selectivity and controllable TZs. *AEU - Int J Electron Commun* 2024;173:154989.
- [9] Wu J, Fu M, Jia D, Feng Q, Xiang Q. A U-band cascaded quadruplet quartz glass SIW filter based on double row vias coupling window. *AEU - Int J Electron Commun* 2024;181:155358.
- [10] Zhang Y, Yao Y, Hu J, He S. A compact and narrow-band bandpass filter based on substrate integrated waveguide and spoof surface plasmon polaritons for millimeter-wave applications. *AEU - Int J Electron Commun* 2024;178:155250.
- [11] Belenguer A, Fernandez MD, Ballesteros JA, de Dios JJ, Esteban H, Boria VE. Compact multilayer filter in empty substrate integrated waveguide with transmission zeros. *IEEE Trans Microw Theory Tech* 2018;66(6):2993–3000.
- [12] Parment F, Ghiotto A, Vuong T-P, Duchamp J-M, Wu K. Air-filled substrate integrated waveguide for low-loss and high power-handling millimeter-wave substrate integrated circuits. *IEEE Trans Microw Theory Tech* 2015;63(4):1228–38.
- [13] Parment F, Ghiotto A, Vuong T-P, Duchamp J-M, Wu K. Ka-band compact and high-performance bandpass filter based on multilayer air-filled SIW. *Electron Lett* 2017;53(7):486–8.
- [14] Nguyen N-H, Ghiotto A, Vuong T-P, Vilcot A, Martin T, Wu K. Dielectric slab air-filled substrate integrated waveguide (SAFSIW) bandpass filters. *IEEE Microw Wirel Compon Lett* 2020;30(4):363–6.
- [15] Casero I, Ballesteros JA, Fernandez MD, Herraiz D, Belenguer A. Easy-to-assemble and high quality-factor ESIW filter with post-based soldered inverters in X-band. *AEU-Int J Electron Commun* 2021;142:153987.
- [16] Bayat-Makou N, Kishk AA. Contactless air-filled substrate integrated waveguide. *IEEE Trans Microw Theory Tech* 2018;66(6):2928–35.
- [17] Amirkabiri A, Idoko D, Bridges GE, Kordi B. Contactless air-filled substrate-integrated waveguide (CLAF-SIW) resonator for wireless passive temperature sensing. *IEEE Trans Microw Theory Tech* 2022;70(7):3724–31.
- [18] Segura-Gómez C, Pérez-Escribano M, Biedma-Pérez A, Palomares-Caballero Á, Padilla P. Contactless AF-SIW phase shifters based on periodic structures at mmwaves. *AEU-Int J Electron Commun* 2024;179:155320.
- [19] Liu Z, Sun D. Transition from rectangular waveguide to empty substrate integrated gap waveguide. *Electron Lett* 2019;55(11):654–6.
- [20] Liu Z, Xu J, Wang W. Wideband transition from microstrip line-to-empty substrate-integrated waveguide without sharp dielectric taper. *IEEE Microw Wirel Compon Lett* 2018;29(1):20–2.

- [21] Ebrahimpouri M, Rajo-Iglesias E, Sipus Z, Quevedo-Teruel O. Cost-effective gap waveguide technology based on glide-symmetric holey EBG structures. *IEEE Trans Microw Theory Tech* 2018;66(2):927–34.
- [22] Santiago D, et al. Robust design of 3D-printed W-band bandpass filters using gap waveguide technology. *J Infrared Millim Terahertz Waves* 2023;44(1):98–109.
- [23] Cameron RJ, Kudsia CM, Mansour RR. *Microwave filters for communication systems: fundamentals, design, and applications*. John Wiley & Sons; 2018.
- [24] Deslandes D, Wu K. Accurate modeling, wave mechanisms, and design considerations of a substrate integrated waveguide. *IEEE Trans Microw Theory Tech* 2006;54(6):2516–26.
- [25] Parment F, Ghiotto A, Vuong T-P, Duchamp J-M, Wu K. Double dielectric slab-loaded air-filled SIW phase shifters for high-performance millimeter-wave integration. *IEEE Trans Microw Theory Tech* 2016;64(9):2833–42.